

Development of Various Photovoltaic-Driven Water Electrolysis Technologies for Green Solar Hydrogen Generation

Sonya Calnan,* Rory Bagacki, Fuxi Bao, Iris Dorbandt, Erno Kemppainen, Christian Schary, Rutger Schlatmann, Marco Leonardi, Salvatore A. Lombardo, R. Gabriella Milazzo, Stefania M. S. Privitera, Fabrizio Bizzarri, Carmelo Connelli, Daniele Consoli, Cosimo Gerardi, Pierenrico Zani, Marcelo Carmo, Stefan Haas, Minoh Lee, Martin Mueller, Walter Zwaygardt, Johan Oscarsson, Lars Stolt, Marika Edoff, Tomas Edvinsson, and Ilknur Bayrak Pehlivan

Direct solar hydrogen generation via a combination of photovoltaics (PV) and water electrolysis can potentially ensure a sustainable energy supply while minimizing greenhouse emissions. The PECSYS project aims at demonstrating a solar-driven electrochemical hydrogen generation system with an area $>10\text{ m}^2$ with high efficiency and at reasonable cost. Thermally integrated PV electrolyzers (ECs) using thin-film silicon, undoped, and silver-doped $\text{Cu}(\text{In,Ga})\text{Se}_2$ and silicon heterojunction PV combined with alkaline electrolysis to form one unit are developed on a prototype level with solar collection areas in the range from 64 to 2600 cm^2 with the solar-to-hydrogen (StH) efficiency ranging from ≈ 4 to 13% . Electrical direct coupling of PV modules to a proton exchange membrane EC to test the effects of bifaciality (730 cm^2 solar collection area) and to study the long-term operation under outdoor conditions (10 m^2 collection area) is also investigated. In both cases, StH efficiencies exceeding 10% can be maintained over the test periods used. All the StH efficiencies reported are based on measured gas outflow using mass flow meters.


1. Introduction

The Paris Agreement target to keep the rise in global temperature below 2.0°C and 1.5°C by 2030 and 2050, respectively, can only be met by substantially reducing fossil fuel use in the transportation, industry, and energy sectors.^[1] The European Green deal pledges to cut greenhouse gas (GHG) emissions by at least 55% , compared with 1990 levels, in 2030. To achieve these targets, it shall be necessary to increase the contribution of renewable energy sources (RES), such as solar and wind, among others, which are carbon neutral, toward electricity generation. Moreover, as the contribution of RES to the energy mix is increased, their intermittent nature requires a corresponding expansion of storage capacity to minimize wastage through curtailment.

S. Calnan, R. Bagacki, F. Bao, I. Dorbandt, E. Kemppainen, C. Schary, R. Schlatmann
PVcomB
Helmholtz-Zentrum Berlin für Materialien und Energie GmbH
Schwarzschildstrasse 3, 12489 Berlin, Germany
E-mail: sonya.calnan@helmholtz-berlin.de

M. Leonardi, S. A. Lombardo, R. G. Milazzo, S. M. S. Privitera
IMM - Institute for microelectronics and microsystems
Consiglio Nazionale Delle Ricerche CNR-IMM
Zona Industriale
Ottava Strada, 5, 95121 Catania, Italy

F. Bizzarri, C. Connelli, D. Consoli, C. Gerardi, P. Zani
Enel Green Power SpA
Viale Regina Margherita, 125, 00198 Roma, Italy

 The ORCID identification number(s) for the author(s) of this article can be found under <https://doi.org/10.1002/solr.202100479>.

© 2021 The Authors. Solar RRL published by Wiley-VCH GmbH. This is an open access article under the terms of the Creative Commons Attribution License, which permits use, distribution and reproduction in any medium, provided the original work is properly cited.

DOI: 10.1002/solr.202100479

M. Carmo, M. Mueller, W. Zwaygardt
Institute of Energy and Climate Research 14 Electrochemical Process Engineering (IEK-14)
Forschungszentrum Jülich GmbH
Wilhelm-Johnen-Str., 52428 Jülich, Germany

S. Haas, M. Lee
Institute of Energy and Climate Research 5 Photovoltaics (IEK-5)
Forschungszentrum Jülich GmbH
Wilhelm-Johnen-Str., 52428 Jülich, Germany

J. Oscarsson, L. Stolt
Solibro Research AB
Vallvägen 5, 75651 Uppsala, Sweden

L. Stolt, M. Edoff, T. Edvinsson, I. B. Pehlivan
Department of Materials Science and Engineering
The Ångström Laboratory
Uppsala University
P.O. Box 35, 75103 Uppsala, Sweden

The use of hydrogen as a means to store excess electricity from RES is gaining traction in the energy system because it can be considered as a net-zero carbon energy carrier.^[2,3] In addition, global demand for H₂ has been continuously increasing as it is an important chemical for both the industrial and transport sectors.^[2] Also, as H₂ does not directly emit GHG, nor other environmentally hazardous substances, it is an important factor in decarbonizing and reducing the overall environmental footprint of the aforementioned sectors. Hydrogen is potentially attractive specifically for the energy and transport sectors, because it can be stored flexibly from over several hours to months, at a time, without the need for “top” up unlike batteries.

A variety of megawatt-scale electrolyzer (EC) plants driven by wind, solar, and hydroelectric energy have been announced and even implemented globally since 2018; however, with a few exceptions, the costs are still less competitive for large off-takers compared with H₂ from conventional fossil fuel plants.^[3–5] In addition, large investments would be needed to adapt and/or expand the existing gas transportation and distribution infrastructure needed for further integration of H₂.^[3,4] However, there is still largely untapped potential for decentralized H₂ generation from RES in the midterm, for smaller consumers, especially in off-grid locations or for self-consumption due to a lack of standards and regulations as well as the relatively high costs. Nevertheless, the global-weighted average levelized cost of electricity (LCOE) of solar photovoltaics (PV) has achieved parity with fossil fuel costs in 2014 and continues to reduce annually due to lower solar PV module prices and reductions in the balance of PV system costs.^[6] Thus, it is to be expected that demonstration of the economic and technical feasibility of PV + EC for smaller applications will stimulate the development of the necessary standards and regulatory frameworks needed for their deployment. Research on small-scale PV + EC systems has centered on simplifying the components, especially in the balance of (EC) plant, to permit modularity and reducing costs. Moreover, despite the relatively high initial investment costs, such units require little or no maintenance and the cost of replenishing the electrolyte is very low compared with that of fuel for diesel generators and thus, may be attractive to users in remote areas.

The most common method to simplify the PV + EC system has been to eliminate power electronics for regulating the input voltage and/or current to the EC in the so-called directly coupled systems. Careful matching of the voltage of the PV and EC can enhance solar-to-hydrogen (StH) conversion efficiencies by up to 50% relatively compared with a system with a DC–DC converter.^[7] However, for MW-scale plants, omitting power electronics is likely less beneficial because their contribution to the total system cost is relatively small and losses in annual gas generation yield caused by long periods of suboptimal coupling may be substantial.^[8]

As the power output of PV modules tends to decrease with increasing operating temperature, while the reverse is true for EC, thermal integration of both subcomponents can be used to benefit from the opposing temperature response. Moreover, thermal integration of the PV modules and ECs allows exclusive use of the incident solar energy to provide both heat and electricity to the EC, thus enhancing the StH efficiency, while maintaining a near-zero carbon footprint.

For example, the PV modules can be cooled by a heat transfer fluid that heats the EC, leading to enhanced StH efficiency.^[9,10]

In another case, the excess heat generated by the PV modules, exposed to concentrated sunlight, is transferred to the EC by direct thermal contact, leading to extremely high StH efficiencies >15–20% but at the cost of more complex engineering and the need for high-temperature-resistant materials.^[11–14] To prevent long start-up times in the morning while the EC is still heating up, or reduced output during low-solar irradiance intervals, such systems would need a heat reservoir. The use of passive heat storage involving covering the EC overnight with insulating jackets to maintain an optimal operating temperature has also been reported, however, also at the cost of increased complexity.^[15]

While photocatalytic (PC) and photoelectrochemical (PEC) devices incorporate direct thermal and electrical integration between the photoactive and catalytic processes, their technical maturity is still low because the photoabsorbing material is in physical contact with the electrolyte, limiting the durability of the device.^[16] In contrast, PV integrated EC, in which the photoabsorber material is physically separated from the electrolyte, have proven to achieve both a higher efficiency and durability than PEC.^[17]

On the basis of the above status quo, the PECSYS project was motivated by the following needs. 1) to scale-up and prove the technical feasibility of directly coupled PV electrolysis systems through in-field testing and 2) to gain a better understanding of the effect of variable solar irradiation and thermal management of systems for direct hydrogen production from sunlight.

2. Background of the PECSYS Approach

The PECSYS project funded by the FCHJU/H2020 program was aimed at demonstrating a 10 m² solar-driven electrochemical hydrogen generation system. Of particular focus was to highlight concepts with levelized cost of hydrogen production below 5 €/kg and to achieve hydrogen production of 16 gH₂/h and thus an StH conversion efficiency of at least 6% with less than 10% decrease in performance after 6 months of continuous operation.

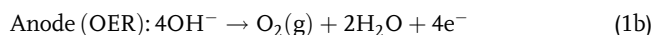
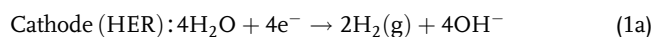
The PECSYS consortium consisted of a multidisciplinary mix of three public research institutes, one university and two manufacturers of commercial PV modules, namely, 1) Helmholtz Zentrum Berlin (HZB), which is a public research center in Germany and whose mission is to conduct user and user-inspired energy materials research for a sustainable, economic, and secure energy system. The HZB was the project coordinator and also developed PV + EC prototypes using direct thermal and electrical integration of silicon (a-Si/c-Si) heterojunction PV modules with alkaline EC. 2) Consiglio Nazionale Delle Ricerche Institute for Microelectronics and Microsystems CNR-IMM (Italy) that conducts research on micronanoelectronics, functional materials and devices, and photonics. It was responsible for investigating the effects of low solar concentration using bifaciality of PV modules on PV + EC systems. 3) Forschungszentrum Juelich, another public research center in Germany, that conducts research to provide comprehensive solutions to the grand challenges facing society in the fields of energy and environment, information, and brain research. The Institute of Energy and Climate Research 5 Photovoltaic (IEK-5) developed devices with direct thermal and electrical integration of thin-film silicon multijunction PV modules with

alkaline EC and characterized the commercial PV modules under standard conditions. The Institute of Energy and Climate research 14 Electrochemical Process Engineering (IEK-14) installed, operated, and monitored the 10 m² PV + EC project demonstrator and also developed the proton exchange membrane (PEM) EC stacks used in the project. 4) Uppsala Universitet, founded in 1477, which is the oldest university in Sweden. The university pursues top-quality research and education and interacts constructively with society, to in different ways contribute to a better world. The Department of Materials Science and Engineering contributed by tuning the properties of silver-doped Cu(In,Ga)Se₂ (ACIGS) to achieve an optimal balance between photovoltage and photocurrent for water splitting and also developed transition metal-based electrocatalysts for alkaline electrolysis. 5) Enel Green Power is a subsidiary of Enel Group, an energy utility corporation headquartered in Italy, that develops and manages power generated from renewable resources worldwide. EGP contributed to the project by developing commercial silicon heterojunction modules that were used in the 10 m² demonstrator. 6) Solibro Research AB located in Sweden, which was the research and development subsidiary of Solibro GmbH, a commercial manufacturer of Cu(In,Ga)Se₂ (CIGS) PV modules, until its insolvency in October 2019. Solibro Research AB developed and provided the commercial CIGS PV modules that were used in the 10 m² demonstrator.

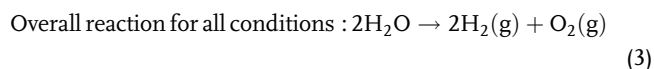
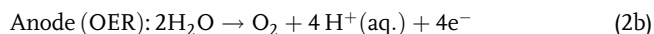
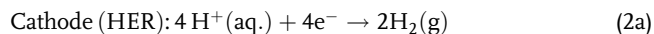
The PECSYS consortium developed low-cost, established PV material modules directly coupled to EC units, enabling a steep learning curve from known PV technologies and Earth-abundant catalysts for alkaline electrolysis. Directly electrically coupled PV electrolysis was favored for reasons already outlined in the Introduction. In addition, this approach was chosen because it is technically feasible in temperate climates unlike concentrated PV or solar thermal hydrogen production and has potentially lower costs.^[18] Further, designs with and without thermal integration of the PV and electrolysis components were investigated, with the former representing a lower technology readiness level (TRL) than the latter.

The electrolysis of water, also referred to as water splitting, is a combination of two half reactions, namely, the hydrogen evolution reaction (HER) and the oxygen evolution reaction (OER), which proceed as follows.

For alkaline conditions



For acidic conditions



Under standard conditions (1 atm and 25 °C), a minimum voltage, E^0 , known as the reversible voltage and corresponding to 1.23 V versus Reversible Hydrogen Electrode = 0 V, is required for the overall reaction. However, for practical electrolysis, a voltage higher

than E^0 is required to drive the anodic and cathodic reactions of the full electrochemical cell as well as to overcome parasitic loads. Thus, the consortium sized the PV modules in such a way as to ensure that the photovoltage over a wide range of operating conditions was sufficient for unassisted overall water splitting in the connected EC. Also, within the project, a generalized PV + EC sizing model was developed based on real device data together with temperature and irradiance climatic data to optimize the annual hydrogen yield for given climatic conditions.^[19]

The performance of the PV + EC prototypes and systems was evaluated by, where possible, individually testing the subcomponents under fixed laboratory conditions and then after integration, by determining the StH efficiency. Laboratory tests were conducted under simulated 1000 W m⁻² solar irradiance (1 sun), while outdoor tests were conducted under fluctuating irradiance conditions and are hereafter termed “real sun.” As most devices were thermally integrated, it was difficult in most cases to stabilize the PV module temperature to 25 °C, the operating temperature during 1 sun characterization varied from one configuration to another. For all the prototypes and systems reported in PECSYS, the StH efficiency η_{StH} (%) with a solar collection area S_{PV} (m²) that operated under an irradiance of G_{photo} (W m⁻²) was calculated using the amount of hydrogen generated \dot{n}_{H_2} in mol/s (determined from collected hydrogen gas flux \tilde{V}_{H_2} , in mL/min, pressure P in bar, temperature T in Kelvin, and the universal gas constant, $R = 8.314 \text{ J}/(\text{K mol})$, as shown in Equation (4)) and the lower heating value (LHV) of hydrogen ($= 237.2 \text{ kJ mol}^{-1}$), as shown in Equation (5).

$$\dot{n}_{\text{H}_2} = \left\{ \frac{P \times \tilde{V}_{\text{H}_2}}{R \times T} \right\} \times 1.67 \times 10^{-3} \quad (4)$$

The conversion factor of 1.67×10^{-3} in Equation (4) is necessary for dimensional correctness as in our case, the units of \tilde{V}_{H_2} have to be converted from mL/min to m³/s and those of P from bar to Pa (equivalent to N m⁻²). This prefactor should be omitted for the general case where SI units are used everywhere.

$$\eta_{\text{StH}} = \left\{ \frac{\dot{n}_{\text{H}_2} \times \text{LHV}}{G_{\text{photo}} \times S_{\text{PV}}} \right\} \times 100\% \quad (5)$$

To compare the productivity of the systems independently of the solar collection area, we define an area-specific H₂ production rate, \dot{m}_{H_2} (g h⁻¹ m⁻²), as the mass of hydrogen collected per hour of operation per square meter of the solar collection area.

3. Results

3.1. Thermally and Electrically Integrated Solar Hydrogen Generation Using Various PV Technologies

The thermally integrated PV EC designs were developed to reduce ohmic losses and transfer excess heat from the PV module to the electrolysis part for enhanced hydrogen generation. We note here that apart from the heat exchange between the PV and electrolysis parts of these devices, no active heating or cooling was used to control the device temperature. This involved starting from lab-scale integrated photoelectrochemical concepts to scale viable concepts to prototype size >100 cm².

3.1.1. Triple-Junction Thin-Film Silicon PV Cells Coupled with Alkaline Electrolysis

At Forschungszentrum Jülich, a scalable 64 cm² aperture area device consisting of triple-junction thin-film a-Si:H/a-Si:H/ μ c-Si:H PV cells coupled with an electrodeposited bifunctional water-splitting NiFeMo catalyst was developed.^[20] Figure 1 shows the scalable design consisting of a repeatable base unit comprising a PV minimodule with an aperture and active area of 64 and

56 cm², respectively, integrated with an EC with electrodes, each sized 26.1 cm². Thus, the device can be scaled arbitrarily without increasing ohmic losses.

This device achieved an StH efficiency of 4.5%_{LHV} with an area-specific H₂ production rate, \dot{m}_{H_2} , of 1.38 g h⁻¹ m⁻². Other performance details are shown in Table 1. We note here that by nature of the design of the electrolysis subcomponents, it was not possible to replicate the same configuration in a

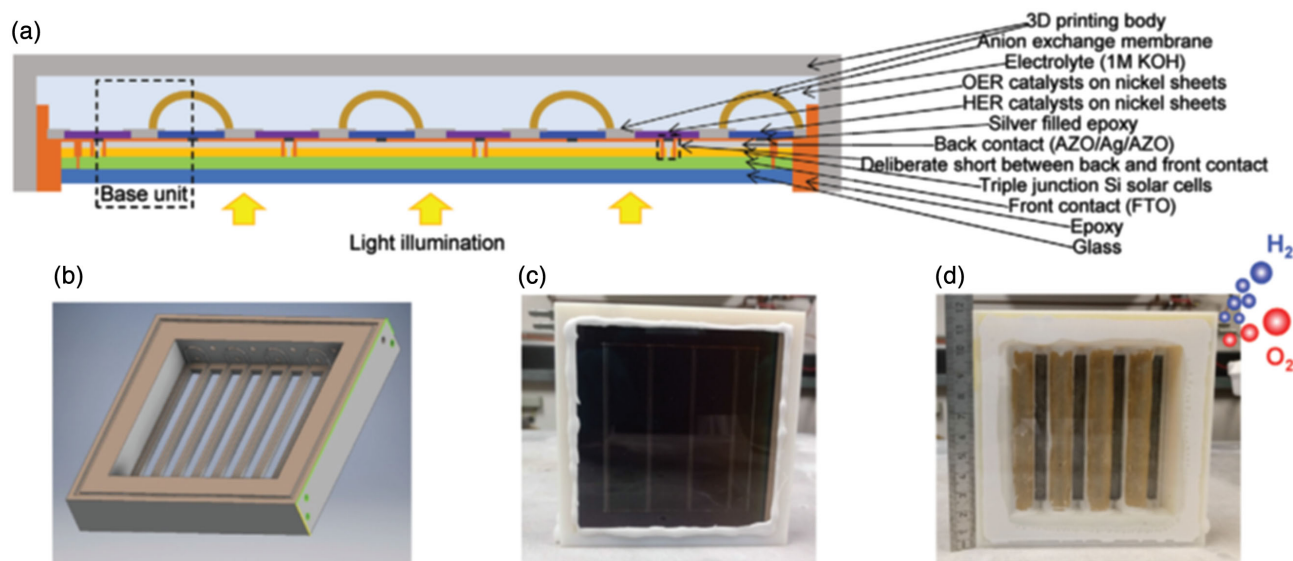


Figure 1. Prototype of the highly integrated and scalable PV + EC device. a) Schematic illustration of the device concept. b) Drawing of the 3D-printed frame used for gas and water management, support for the catalyst, the PV module, and the membranes. c,d) Photographs of prototypes with (c) front-side view (PV side) and (d) back-side view (EC side). Reproduced with permission under the terms of the Creative Commons CC BY license.^[20] Copyright 2020 The Authors. Published by WILEY-VCH.

Table 1. Performance of thermally integrated PV electrolysis prototypes investigated in the PECSYS project tested at 1000 W m⁻² as of December 2020 and presented in Section 3.1. Performance is determined by the amount of collected hydrogen, at ≈ 1 bar, measured by the H₂ production rate in terms of volume or solar collection area specific mass (\bar{V}_{H_2} and \dot{m}_{H_2}). The operating temperature was variable for all devices except where indicated.

PV approach	Thin-film silicon ^[20]	ACIGS (1) ^[21]	ACIGS (2.1)	ACIGS (2.2)	Silicon heterojunction ^[22]	Silicon heterojunction	PV approach
Section	3.1.1	3.1.2	3.1.2	3.1.2	3.1.3	3.1.3	Section
PV collection area, active/total (cm ²)	56/64	78/100	78/101	82.3/100	228/294	2480/2600	PV collection area, active/total (cm ²)
PV module efficiency, (%)	-/-	16.1	14.3	17.3	17.1 ^{a)}	17.6 ^{a)}	PV module efficiency (%)
Catalysts	Bifunctional NiMoFe	NiMoV(cathode)-NiO(anode)	Bifunctional NiFe (LDHs) ^{b)}	Bifunctional NiFe (LDHs)	NiMo (cathode)-NiFeO (anode)	NiMo (cathode)-NiFeO (anode)	Catalysts
Duration of operation (h)	0.5	100	168	12	75	≈ 50	Duration of operation (h)
Max. ^{c)} StH efficiency, (% _{LHV})	4.7 ^{c)}	9.1 ^{d)}	10 ^{d)}	13.4 ^{d)}	10 ^{a)}	7 ^{a)}	Max. StH efficiency (% _{LHV})
Avg. ^{e)} StH efficiency (% _{LHV})	4.5 ^{d)}	8.5 ^{d)}	9.7 ^{d)}	11.3 ^{d)} (average)	3.5 ^{a)} at 25 °C (1-sun);	5.1 ^{a)}	Avg. StH efficiency (% _{LHV})
Avg. \bar{V}_{H_2} (mL/min)	1.7	3.3	5.4	5.74	7.9	85	\bar{V}_{H_2} (mL/min)
Avg. \dot{m}_{H_2} g (h m ²) ⁻¹	1.38	2.75	2.87	3.74	1.07	1.56	\dot{m}_{H_2} g (h m ²) ⁻¹

^{a)}Using total PV area; ^{b)}LDH: layered double hydroxides; ^{c)}Max. short for maximum; ^{d)}Using active PV area as integration made a significant portion of the photoabsorber to photovoltaically inactive; ^{e)}Avg. short for average.

standalone EC to compare the operation with and without thermal integration of the PV cells and EC cells.

3.1.2. Silver-Doped $\text{Cu}(\text{In,Ga})\text{Se}_2$ PV Cells Coupled with Alkaline Electrolysis

At Uppsala University and Solibro Research AB, a scalable thermally integrated PV alkaline electrolysis device was designed using ACIGS and precious metal-free electrocatalysts. The schematic design and photograph of the integrated ACIGS + EC device are shown in Figure 2. Continuous optimization of the catalysts and the device layout^[21] gradually improved the performance, as shown in Table 1. The final prototype (Type 2.2) achieved an average StH efficiency, under 1000 W m^{-2} illumination, of $11.3\%_{\text{LHV}}$ (maximum value of $13.5\%_{\text{LHV}}$ corresponding to an \dot{m}_{H_2} of $3.7 \text{ g h}^{-1} \text{ m}^{-2}$ for the active area of 82.2 cm^2). This prototype was later on installed in the demonstrator testbed in Juelich and in November 2020, an average StH efficiency of $10\%_{\text{LHV}}$ was recorded.

3.1.3. Silicon-Based Heterojunction PV Module Coupled with Alkaline Electrolysis

The final thermally integrated PV EC approach was developed at the Helmholtz Zentrum Berlin using a-Si/c-Si heterojunction PV cells and an alkaline EC. The first prototype had a solar collection area of 294 and 50 cm^2 geometric electrode area (Figure 3a). The EC electrodes consisted of NiMo and NiFeO on Ni foam substrate for the HER and the OER, respectively, with Zirfon membrane (UTP 500) acting as the gas separator. The device was characterized both outdoors (real sun) and indoors at 1 sun (1000 W m^{-2}) using a solar simulator.^[22] The device operated for about 75 h and spent about 145 h connected to the measurement system and filled with electrolyte (1.0 M KOH).

Thanks to insights from the analysis of outdoor performance of the aforementioned prototype, a larger one (2600 cm^2 collection area, see Figure 3b) was developed and tested. The heat transfer was improved by circulating the electrolyte through a heat exchange chamber inserted between the PV module and the EC, before feeding the EC. This prototype has a simpler balance of plant than others^[9,10] because it eliminates both the need for a separate fluid circulation circuit for heat transfer and power conditioning electronics. Unlike the previous prototype for which the EC could not be separately tested, the output of the prototype

could be tested with and without thermal integration. The current voltage curves measured separately for the PV module and the EC stack at 1 sun under different device temperatures are omitted here because of space limitations. However, we briefly show an example of the effect of thermal integration under simulated 1 sun illumination, as shown in Figure 3c,d. A comparison of the hydrogen and oxygen flow rates, as well as the operating current as a function of time for 1000 W m^{-2} , is shown in figure 3d. It can be seen that after 60 min of operation the hydrogen flow rate with and without thermal integration was 85 and 40 mL min^{-1} . An analogous relative enhancement by thermal integration was also evident in the oxygen flow rate and operating current. The H_2/O_2 ratio was close to 2:1 in both measurements. Similarly, the transients of the values of StH efficiency determined using the collected H_2 volume and the operating current showed enhancement by thermal integration of the PV module with the EC stack. With thermal integration, the Faradaic efficiency is somewhat lower than 100% due to possible engineering issues including loss of H_2 gas to the atmosphere. Finally, the temperature transients in Figure 3e show that, with thermal integration, an appreciable amount of heat is transferred between the two components and after 60 min, the PV temperature is reduced, whereas the electrolyte temperature is increased compared with the case without thermal integration. A detailed analysis of this prototype shall be presented in other studies. Thus, for the 2600 cm^2 prototype, a 34% relative improvement compared with the 290 cm^2 -sized one, in StH efficiency to 5.1% at 1000 W m^{-2} , was achieved, by the end of the project in December 2020. Under these conditions, the scaled-up prototype achieved a H_2 -generating capacity of 85 mL min^{-1} at an \dot{m}_{H_2} of $1.56 \text{ g h}^{-1} \text{ m}^{-2}$. In the meantime, further postproject improvements have enhanced the StH efficiency to $6.1\%_{\text{LHV}}$ and a H_2 -generating capacity of 100 mL min^{-1} , under simulated 1 sun conditions test conditions at 1000 W m^{-2} , while StH reaches 10% in outdoor (real sun) conditions (details to be presented in other studies).

The performances of the thermally integrated PV electrolysis prototypes shown in Figure 1–3 are shown in Table 1. Generally, the StH efficiency of these thermally integrated approaches can be further improved by increasing the PV minimodule efficiency, minimizing loss in efficiency associated with integration and scale-up. The aforementioned aspects as well as the durability of the electrolysis part require further research.

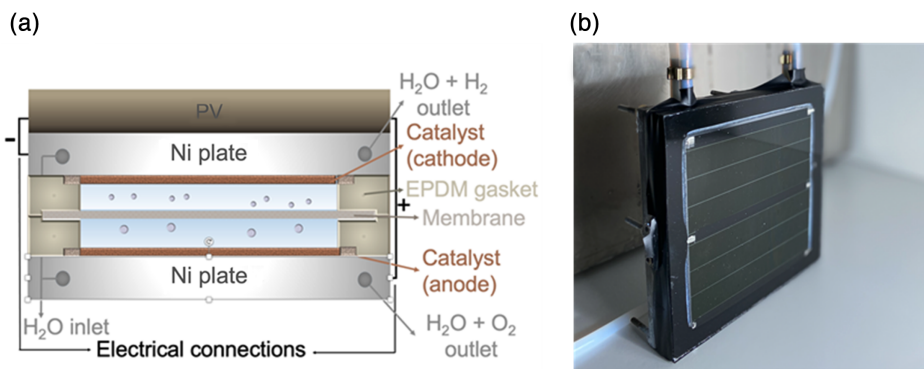


Figure 2. a) Schematic and b) photograph of the ACIGS PV minimodule with an area of 100 cm^2 in direct contact with a thin EC with 100 cm^2 catalyst area.

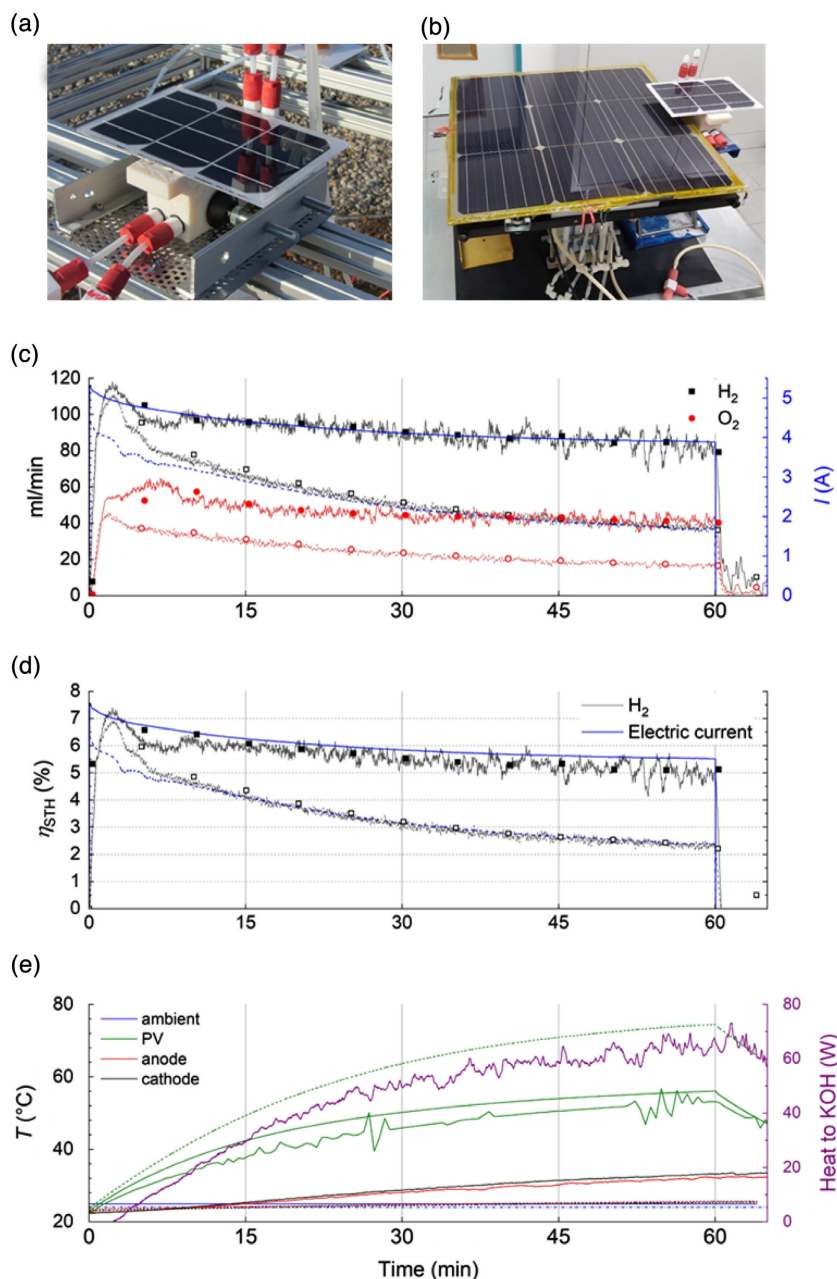


Figure 3. a) Si heterojunction PV + EC integrated device (294 cm² collection area) in an outdoor test setup. The liquid alkaline EC is inside the white plastic casing below the PV module. b) Scaled-up prototype (2600 cm²) with heat exchanger placed between EC and PV module to improve heat transfer. The time transients of different parameters measured for the 2600 cm² collection area prototype under simulated 1 sun illumination with (continuous curves and/or solid symbols) and without (dotted and/or unfilled symbols) thermal integration c) for hydrogen flow rate, oxygen flow rate, and operating electrical current; d) StH conversion efficiency η_{STH} calculated from the collected hydrogen volume flow rate and the measured operating current and the ambient temperature, the PV module temperature, the average electrolyte temperature on the anode and cathode side, as well as the heat transferred to the KOH electrolyte.

3.2. Solar Hydrogen Generation Using PV Modules Directly Coupled to PEM EC with Balance of Plant Innovations

The second category of PV + EC systems consisted of PV modules directly electrically coupled to PEM EC, but in this case, they were thermally “decoupled.” Uniquely in the PECSYS

project, the balance of plant for the EC was minimized^[23] by 1) feeding water to the EC from the cathode side only; 2) using hydraulics (siphoning effect) and not pumps to provide feed water to the EC; 3) eliminating power management electronics; and 4) eliminating active heating/cooling of the EC.

3.2.1. Bifacial Silicon Heterojunction PV Module Coupled with PEM Electrolysis

In the first system, we studied the effect of using bifacial instead of monofacial silicon heterojunction PV minimodules on the hydrogen yield. In this setup, a 730 cm² minimodule consisting of three amorphous Si/crystalline Si heterojunction cells with a bifaciality factor of $\approx 90\%$ and an output voltage exceeding 1.5 V was developed by Enel Green Power at its 3SUN facility. These PV cells were manufactured using an industrial setting, as reported in the study by Condorelli.^[24] The PV cells were manually assembled into a module which was then directly connected to a single PEM electrolysis cell developed at FZJ and tested under outdoor conditions at CNR. The PV module layout, height, and orientation at the experimental site were chosen to optimize bifaciality, using a 3D bifacial performance optimization model.^[25] The PV module was oriented to south with an inclination of 35°, optimized for the latitude of Catania, Italy (37°31'N, 15°4'E), and the system setup is shown in **Figure 4**.

Low solar concentration was achieved via an albedo effect of about 30% combined with a bifacial factor of 90%. Compared with a-Si/c-Si heterojunction PV minimodule with monofacial



Figure 4. Direct solar hydrogen generation system consisting of a three-cell bifacial silicon heterojunction PV module directly coupled to a single PEM EC cell at Catania, Italy.

irradiance collection, the bifacial setup resulted in a 17% relative increase in StH efficiency to 13.5%_{LHV} for an average production rate of 4.2 g h⁻¹ m⁻² for irradiance levels between 800 and 1200 W m⁻². This system also showed stable outdoor operation for 55 h and a detailed account of the performance behavior can be found in the study by Privitera et al.^[26]

3.2.2. Commercial PV Modules Coupled with PEM Electrolysis in a 10.3 m² Array

The second system made up the final project demonstrator for direct solar hydrogen generation, with a PV collection area greater than 10 m². The demonstrator was installed at an outdoor test field located at the FZJ (50°55' N, 6° 21' E) in Juelich, Germany, in the beginning of 2020, as shown in **Figure 5a**. The 10 m² PV array consisted of eight CIGS PV modules from Solibro Research AB and three a-Si/c-Si heterojunction PV modules, from Enel Green Power, connected directly to PEM EC stacks developed at FZJ. Each PV module (with the exception of two a-Si/c-Si heterojunction modules which were connected in series to form one unit) was directly coupled to a dedicated EC stack in the so-called cassette configuration, as shown in **Figure 5b**. Each of these PV + EC cassettes formed a unique modular solar-to-hydrogen generating unit, as also described in other studies.^[23,27] One advantage of this configuration is that the sizing of the plant could be flexibly changed by varying the number of modular units in an array.

The demonstrator was commissioned in January 2020 and continuously operated from April to November 2020. The amount of hydrogen collected from each modular PV + EC unit was totaled for the whole plant and used to calculate StH using the expression in Equation (1). The system achieved average StH efficiency of 10%_{LHV} over 9 months operation (equivalent to 6480 h) and a total of 22 kg of hydrogen were collected in this time with a performance degradation of less than 10%, exceeding the respective project targets.

3.3. Electrocatalysts for Electrolysis of Water (Water Splitting) Developed in the PECSYS Project

While the technological development of PV modules used in the PECSYS project was already well established at the beginning of the project, this was not the case for electrocatalysts which are

(a)



(b)

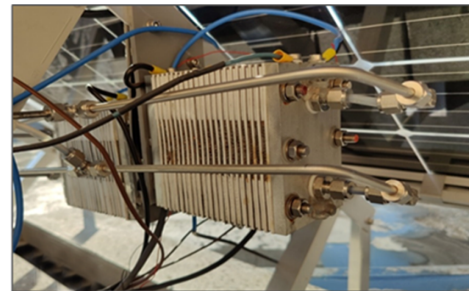


Figure 5. a) Aerial view of the final setup of the 10 m² demonstrator plant at Forschungszentrum Juelich, Germany. b) Photograph showing a PEM EC stack directly mounted onto the back of one of the a-Si/c-Si heterojunction PV modules in a cassette design.

essential for water electrolysis. Also, one of the goals of the project was to reduce the costs for which minimizing or eliminating the use of platinum group metals (PGMs) would play a role. Thus, although this was not at the focus of the PECSYS objectives, a lot of research was done in developing Earth-abundant electrocatalysts and on sizes that are not usually reported in the literature, and these developments were very useful in the success of the project. A summary of the performance of these catalysts in comparison with the best in class catalysts is shown in Table 2. It can be seen that the catalysts developed in PECSYS perform as well as are the state of the art and have moreover been tested in devices, in some cases, even under harsh operating conditions.

The platinum group catalysts used for PEM EC in the PECSYS project are omitted from Table 3 for brevity and also as their high performance is generally well established.^[28]

4. Discussion

4.1. Summary of Results and Comparison with the State of the Art

A schematic that summarizes the results of the different PV + EC approaches investigated within the PECSYS project is shown in Figure 6.

The detailed performance of the larger systems operated under real sun conditions in comparison with similar-sized

systems developed in the past 10 years and reported in other studies^[29,30] is shown in Table 3. In particular, the demonstrator was operated for a longer time period, a total of 9 months or 6480 h, than other systems for which typically direct PV-to-EC coupling is only studied on a short-term basis.

Figure 7 shows a comparison of the StH efficiency, of different directly coupled PV + EC devices, as well as PC and hybrid PEC-PV + EC devices, as a function of the solar collection aperture area. Data from reports on devices smaller than 1 cm² and/or tested with concentrated solar irradiance are omitted for clarity. The datapoints of devices for which StH efficiency was determined using the operating current and using the amount of gas collected are shown in Figure 7a,b, respectively. The datapoints corresponding to the devices developed in this work are labeled with the respective section numbers, whereas those from literature are labeled with the respective references. It can be seen that the thermally integrated prototypes in PECSYS achieved comparable and even higher performance for simulated 1 sun irradiance, than has been reported for devices using abundant active materials and for similar size. In addition, even for the directly coupled PV module + EC stack systems, without thermal integration and with solar collection areas above 1 m² (= 10⁴ cm²), the PECSYS demonstrator shows the highest average StH efficiency above 10%_{LHV}. Note that the low StH values of less than 1.0%_{LHV} all belong to devices based on PEC^[31–33] or PC^[34,35] technologies and are a result of the material and/or

Table 2. Comparison of Earth-abundant catalysts developed in PECSYS tested at 25 °C in alkaline conditions, with the best in class state of the art.

HER						
Catalyst material	NiFeMo	NiMo	NiFe LDH	NiMo	NiMo	Catalyst material
Electrode	Nickel sheet	Nickel foam	Nickel foam	Nickel foam	Glassy carbon	Electrode
Preparation method	ED ^{a)}	Sputtering	HP ^{b)}	ED	ED	Preparation method
Deposition size (cm × cm)	8.2 × 0.8	10 × 10	10 × 10	15 × 15	0.5 disc diam. ^{c)}	Deposition size (cm × cm)
Overpotential at 10 mA cm ^{−2} (V)	320 @ 50 mA cm ^{−2} (3 × 1 cm)	94 (1 × 1 cm)	189 (1 × 1 cm)	92 ± 22 (1 × 1 cm)	40 (0.5 cm diam.)	Overpotential at 10 mA cm ^{−2} (V)
Proven in device	Yes, Figure 1	Yes	Yes, Figure 2	yes, Figure 3b	no	Proven in device
Reference	[20]	[21]	This work	This work	[28]	Reference
OER						
Catalyst material	NiFeMo	NiMo	NiFe LDH	NiFeO	Ru	Catalyst material
Electrode	Nickel sheet	Nickel foam	Nickel foam	Nickel foam	Glassy carbon	Electrode
Preparation method	ED	Sputtering	HP	ED	ED	Preparation method
Deposition size (cm × cm)	8.2 × 0.8	10 × 10	10 × 10	15 × 15	0.5 Disc diameter	Deposition size (cm × cm)
Overpotential at 10 mA cm ^{−2} (V)	330 @ 50 mA cm ^{−2} (3 × 1 cm)	94 (1 × 1 cm)	200 (1 × 1 cm)	266 ± 1 (1 × 1 cm)	290	Overpotential at 10 mA cm ^{−2} (V)
Proven in device	yes, Figure 1	yes	yes, Figure 2	yes, Figure 3b	no	Proven in device
Reference	[20]	[21]	This work	This work	[28]	Reference

^{a)}ED: electrodeposition; ^{b)}HP: hydrothermal process; ^{c)}Diam: diameter.

Table 3. Comparison of the outdoor performance solar hydrogen generation systems using PV modules directly coupled to PEM ECs. Hydrogen gas was collected at ≈ 1 bar.

Parameter						Parameter
Location	Catania (IT)	Catania (IT)	Juelich (DE)	Thawul (SA)	Tsukuba (JP)	Location
PV technology	Monofacial silicon heterojunction	Bifacial silicon heterojunction + 30% albedo effect	CuInGaSe and silicon heterojunction	Polycrystalline silicon	Polycrystalline silicon	PV technology
PV collection area (m ²)	0.073	0.073	10.3	1.5	21.5	PV collection area (m ²)
PV nominal power [kW _{el}]	0.134	0.120	1.73	0.27	2.6	PV nominal power [kW _{el}]
Avg. ^{a)} StH efficiency, (% _{LHV})	11.5	13.5	10–11	9.4	$\approx 5.0^b$	Avg. StH efficiency (% _{LHV})
\dot{m}_{H_2} g/(h·m ²)	-/-	4.2	2.3	1.2	-/-	\dot{m}_{H_2} g/(h·m ²)
Outdoor operation (h)	-/-	≈ 100	6480	10	20	Outdoor operation (h)
Reference	[26]	[26]	This work	[29]	[30]	Reference

^{a)}Avg. is short for average; ^{b)}Calculated from information provided in the respective publication.

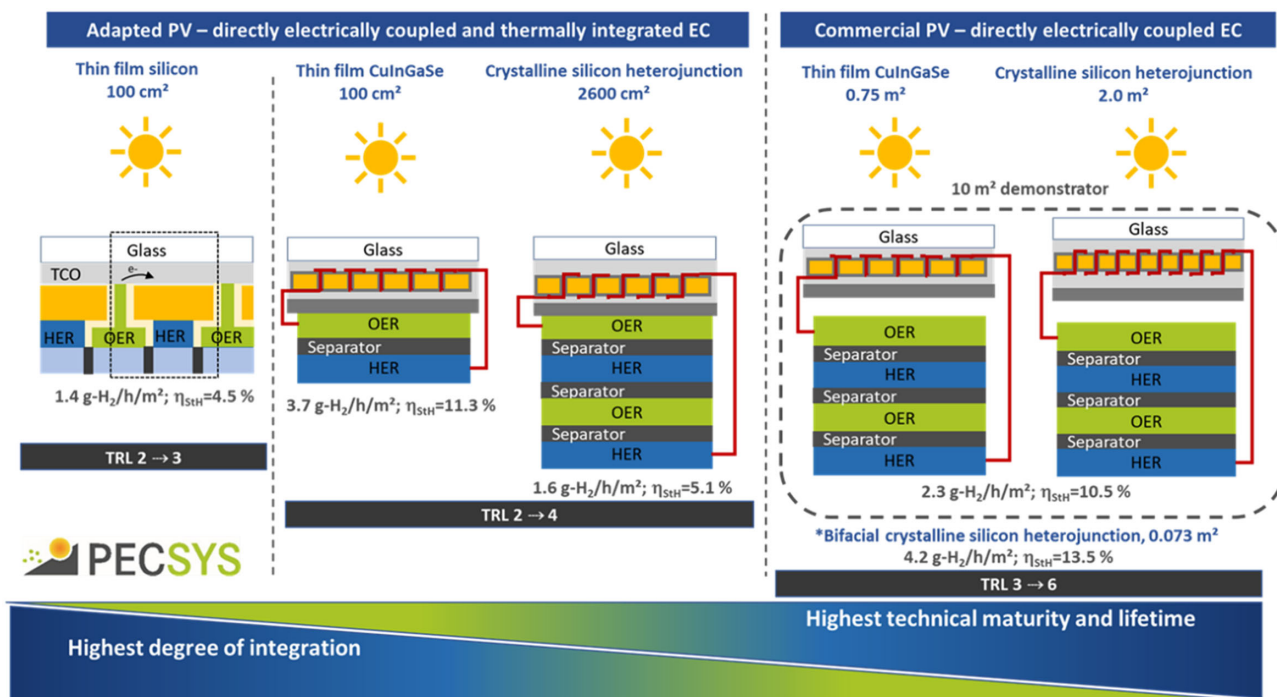


Figure 6. Summary of directly coupled PV electrolysis systems investigated in PCSYS spanning different levels of integration as well as technical maturity measured via the TRL.

technological limitations such as low electronic quality and/or lack of suitable device approaches that limit photocorrosion. However, some progress in StH efficiency and scale (e.g., 3% LHV for a solar collection area of 1.6 m² or 16 × 10³ cm²) is apparent especially when PEC devices are combined with crystalline silicon-based PV.^[36] Nevertheless, high average values of StH efficiency approaching or beyond 10% LHV for devices with a solar collection area of 100 cm² or greater, despite a significant presence of systems developed in the PCSYS project, are still dominated by EC using PGMs (also in Figure 7b).^[37–52]

4.2. Prospects for Application

The PCSYS technical approach using the direct coupling of PV modules to an EC stack is an interesting starting point for further development to fulfill the needs of green hydrogen production at a commercial- and industrial-scale level (among others). Such configurations, that omit the power conditioning of the EC, are alternatives to the currently used ones, in which the EC is fed using electricity from grid and green sources via AC/DC, DC/AC, and DC/DC converters and transported by kilometers

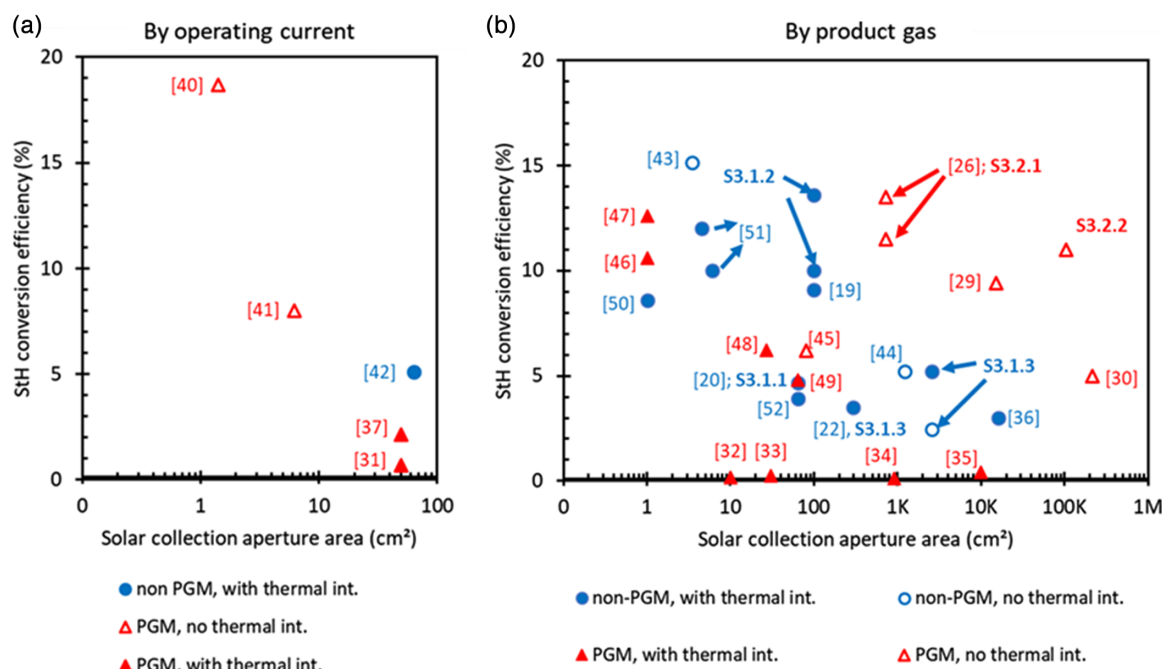


Figure 7. StH conversion efficiency, determined from the a) operating current and from b) the amount of product gas collected as a function of the PV aperture area for different devices. The data in each graph are grouped according to whether or not the electrocatalysts used contain PGM and, whether or not the PV and electrolysis devices are thermally integrated. The data points corresponding to the devices developed in within this work are labeled using the sections in which they are presented, whereas data points from the literature are labeled with the reference number. All data are reported for non-concentrated solar irradiance and all devices with a solar collection of 730 cm² and above (except 2600 cm²) were measured under real sun conditions and thus more accurately portray average StH values, whereas the rest were measured under simulated 1 sun (1000 W m⁻²) conditions and portray maximum or initial StH values. Note that device operating temperatures may vary.

of lines with the related losses. In the near and midterm, application of the PECSYS approach in the decentralized hydrogen production for storage of PV electricity for capacities in the 1–10 s of kW range, for example, for residential or small commercial user/producers, already seems possible. The approach used in the 10 m² demonstrator, if economically scaled to 0.1–10 s of MW capacity, may be a basis for distributed solar-based green hydrogen industrial production for refineries as well as fertilizer and steel manufacturers, which use large amounts of hydrogen (see Figure 8). Other potential end users could be entities in the chemical and industrial sectors that intend to decarbonize their processes. In addition, with slight modifications to such hybrid PV hydrogen generation plants, the energy production can be modulated between electrical energy delivered to the power grid and H₂ production, providing also grid balance services, as shown by the gray area. By improving and demonstrating a sufficient system reliability, we think that it is realistic to reach a solar green hydrogen cost below 5 €/kg-H₂ in sunny locations.

4.3. Learnings from the Project

The PECSYS project activities produced a number of results that are of significant scientific and technological interest to the green hydrogen community. As already outlined, different configurations and approaches were considered, leading to a diversity of results that also provided some insights that allow for generalization of some conclusions for directly coupled PV electrolysis

systems for solar hydrogen generation. These results showed that hydrogen generation under real-world conditions with directly coupled PV electrolysis under 1 sun is feasible even with a much reduced balance of system, provided that the components are optimally matched. Moreover, the elimination of power conditioning, active heating/cooling, and pumps reduces the capital costs and energy required for ancillary services. The directly coupled devices have a compact design with a maximum of four terminal connections for electrolyte feed and gas collection and minimal to no wiring, enabling modular installation. Scaling of the hydrogen-generating system can be done by simply adding or reducing the number of modules in an array as required, in a similar way to conventional PV panels. Moreover, performance loss of an entire array as a result of partial shading can be mitigated as unaffected panels continue to generate hydrogen at the maximum possible rate for a given irradiation level.

The use of Earth-abundant catalysts combined with low-cost PV absorber materials can be used to scale thermally integrated devices with efficiencies that are comparable with those obtained using more expensive materials, provided that device durability can be guaranteed. We were also able to demonstrate that heat exchange between the PV and electrolysis module does indeed boost StH efficiency.

There were also some challenges faced and these provide directions for further research, especially in improving the EC as well as the integration designs. As the EC's hydrogen production rate directly follows the changes in the incident irradiance, any system with a PV module directly coupled to an EC would

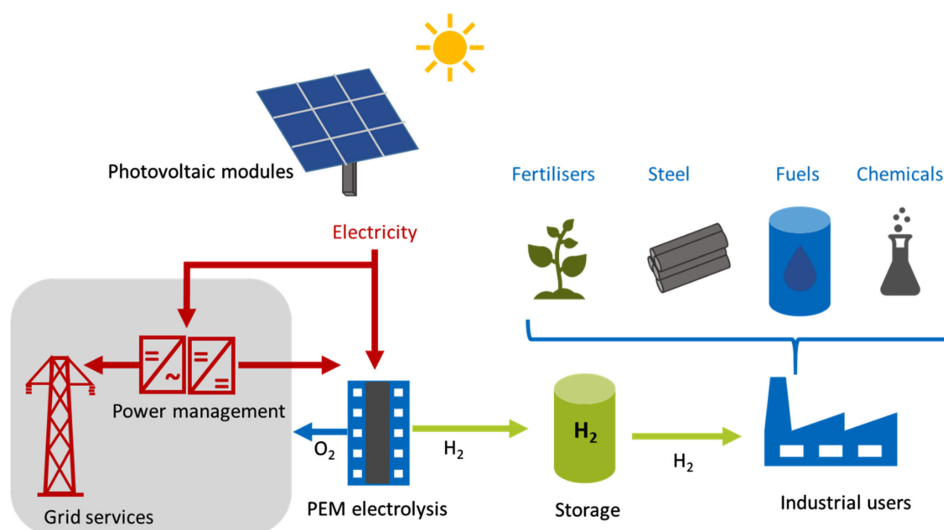


Figure 8. Reference configuration for the envisaged system for distributed hydrogen production for industrial stakeholders, based on the current PECSYS technology. The shaded area shows an alternative hybrid configuration with switching power electronics to optimize revenue streams at an industrial level.

require a buffer to stabilize the supply of hydrogen to downstream equipment such as compressors and fuel cells. Also, operating classically designed cells without power electronics control requires a safety mechanism or the use of a recombination catalyst on the anode side, to prevent danger of explosion due to hydrogen cross-over, at extremely low current densities, that can occur during periods of low solar irradiance. The operation of electrolysis at close to atmospheric pressure reduces safety concerns but comes at a cost of compressing the hydrogen to pressures of at least 25–30 bar (comparable with the output of steam methanol reforming). Also, although the PV module lifetime is quite high, the EC lifetime has to be further improved.

Especially challenging for the thermally integrated systems is the hermetic sealing of the device to prevent the leakage of both gases and electrolyte when one of the joints is made up of glass.^[53] The updated silicon heterojunction PV integrated alkaline EC design relaxes this constraint as the sealing closest to the PV module is only required to prevent leakage of the electrolyte from the heat exchanger, allowing more robust hermetic sealing of the EC against gas leakage using compression screws.

The life cycle impact (not presented here) could only be estimated as some manufacturing steps for the EC are not yet standardized and information on component production (automation, scaling, standards, etc.) and supply chains is still limited.

This work can, in the first instance, be extended by increasing the efficiency, scale, reliability, and lifetime of the system. Further, holistic studies to optimize both the location and size for an off-grid solar/hydrogen energy system consider social, economic, technical, and environmental factors.^[54] Finally, the benefit of thermal integration under subzero temperature conditions should be investigated as suggested by a recent study.^[55]

5. Conclusion

In the PECSYS project several approaches for direct coupling of PV and electrolysis for direct solar hydrogen production were

investigated, spanning different levels of technical maturity and component integration. We have shown that thermal integration does boost efficiency and H₂ production and these results have also provided a better understanding of the scale-up challenges and operation behavior of thermally integrated PV ECs that could be applied to PEC and PC technologies.

In general, for each approach considered, we achieved efficiency and capacity values among the best in class for each approach. However, we note that for all concepts, the durability of the ECs requires more research and further scale-up is required to approach higher technological maturity. Such further research and development is anticipated to lead to a targeted H₂ production cost in the range of 2.5–5.5 €/kg or even better.

Acknowledgements

The PECSYS project received funding from the Fuel Cells and Hydrogen 2 Joint Undertaking under grant agreement no. 735218. This joint undertaking receives support from the European Union's Horizon 2020 Research and Innovation programme and Hydrogen Europe and N.ERGHY. The project started on January 1, 2017, with a duration of 48 months. The affiliations were corrected on September 27th, 2021.

Open access funding enabled and organized by Projekt DEAL.

Conflict of Interest

The authors declare no conflict of interest.

Data Availability Statement

Research data are not shared.

Keywords

direct coupling, direct solar hydrogen generation, low-temperature electrolyzers, photovoltaic-driven water electrolysis

Received: June 30, 2021
Revised: August 22, 2021
Published online: September 22, 2021

- [1] *Global Warming of 1.5°C: An IPCC Special Report on the impacts of global warming of 1.5°C above pre-industrial levels and related global greenhouse gas emission pathways, in the context of strengthening the global response to the threat of climate change, sustainable development, and efforts to eradicate poverty*, Intergovernmental Panel on Climate Change (IPCC), World Meteorological Organization, Geneva, Switzerland **2018**.
- [2] *World Energy Investment 2019*, International Energy Agency (IEA), Paris **2019**, www.iea.org/wei2019/ (accessed: June 2021).
- [3] *Hydrogen: A renewable energy perspective*, International Renewable Energy Agency IRENA, Abu Dhabi **2019**.
- [4] *The Future of Hydrogen: Seizing today's opportunities*, International Energy Agency (IEA) **2019**, <https://www.iea.org/reports/the-future-of-hydrogen> (accessed: June 2021).
- [5] C. Wulf, P. Zapp, A. Schreiber, *Front. Energy Res.* **2020**, *8*, 191.
- [6] *Renewable Power Generation Costs in 2018*, International Renewable Energy Agency (IRENA), Abu Dhabi **2019**.
- [7] T. L. Gibson, N. A. Kelly, *Int. J. Hydrogen Energy* **2008**, *33*, 5931.
- [8] G. M. Sriramagiri, W. Luc, F. Jiao, K. Ayers, K. D. Dobson, S. S. Hegedus, *Sustainable Energy Fuels* **2019**, *3*, 422.
- [9] M. Gül, E. Akyüz, *Energies* **2020**, *13*, 2997.
- [10] S. Senthilraja, R. Gangadevi, H. Koeten, R. Marimuthu, *Heliyon* **2020**, *6*, 05271.
- [11] G. Peharz, F. Dimroth, U. Wittstadt, *Int. J. Hydrogen Energy* **2007**, *32*, 3248.
- [12] A. Nakamura, Y. Ota, K. Koike, Y. Hidaka, K. Nishioka, M. Sugiyama, K. Fujii, *Appl. Phys. Express* **2015**, *8*, 107101.
- [13] A. Fallisch, L. Schellhase, J. Fresko, M. Zedda, J. Ohlmann, M. Steiner, A. Bösch, L. Zielke, S. Thiele, F. Dimroth, T. Smolinka, *Int. J. Hydrogen Energy* **2017**, *42*, 26804.
- [14] S. Tembhurne, F. Nandjou, S. Haussener, *Nat. Energy* **2019**, *4*, 399.
- [15] D. Scamman, H. Bustamante, S. Hallett, M. Newborough, *Int. J. Hydrogen Energy* **2014**, *39*, 19855.
- [16] D. Bae, B. Seger, P. C. K. Vesborg, O. Hansen, I. Chorkendorff, *Chem. Soc. Rev.* **2017**, *46*, 1933.
- [17] J. H. Kim, D. Hansora, P. Sharma, J.-W. Jang, J. S. Lee, *Chem. Soc. Rev.* **2019**, *48*, 1908.
- [18] T. Grube, J. Reul, M. Reuß, S. Calnan, N. Monnerie, R. Schlatmann, C. Sattler, M. Robinius, D. Stolten, *Sustainable Energy Fuels* **2020**, *4*, 5818.
- [19] I. Bayrak Pehlivan, U. Malm, P. Neretnieks, A. Gluesen, M. Mueller, K. Welter, S. Haas, S. Calnan, A. Canino, R. G. Milazzo, S. M. S. Privitera, S. A. Lombardo, L. Stolt, M. Edoff, T. Edvinsson, *Sustainable Energy Fuels* **2020**, *4*, 6011.
- [20] M. Lee, B. Turan, J. P. Becker, K. Welter, B. Klingebiel, E. Neumann, Y. J. Sohn, T. Merdzhanova, T. Kirchartz, F. Finger, U. Rau, S. Haas, *Adv. Sustainable Syst.* **2020**, *4*, 202000070.
- [21] I. B. Pehlivan, J. Oscarsson, Z. Qiu, L. Stolt, M. Edoff, T. Edvinsson, *iScience* **2021**, *24*, 101910.
- [22] E. Kemppainen, S. Aschbrenner, F. Bao, A. Luxa, C. Schary, R. Bors, S. Janke, I. Dorbandt, B. Stannowski, R. Schlatmann, S. Calnan, *Sustainable Energy Fuels* **2020**, *4*, 4831.
- [23] M. Müller, W. Zwaygardt, E. Rauls, M. Hehemann, S. Haas, L. Stolt, H. Janssen, M. Carmo, *Energies* **2019**, *12*, 4150.
- [24] G. Condorelli, W. Favre, M. Sciuto, A. Ragonesi, P. Rotoli, A. Di Matteo, D. Nicotra, F. Rametta, D. Iuvara, M. Foti, A. Daniel, L. Sicot, V. Bath, A. Derrier, Y. Veschetti, C. Roux, P.-J. Rebeyron, C. Gerardi, in *Proc. 47th IEEE Photovoltaic Specialists Conf. (PVSC)*, IEEE, Piscataway, NJ **2020**, pp. 1702–1705.
- [25] F. Ricco Galluzzo, P. E. Zani, M. Foti, A. Canino, C. Gerardi, S. Lombardo, *Energies* **2020**, *13*, 869.
- [26] S. M. S. Privitera, M. Müller, W. Zwaygardt, M. Carmo, R. G. Milazzo, P. Zani, M. Leonardi, F. Maita, A. Canino, M. Foti, F. Bizzarri, C. Gerardi, S. A. Lombardo, *J. Power Sources* **2020**, *473*, 228619.
- [27] M. Müller, M. Carmo, A. Glösen, M. Hehemann, S. Saba, W. Zwaygardt, D. Stolten, *Int. J. Hydrogen Energy* **2019**, *44*, 10147.
- [28] C. C. L. McCrory, S. Jung, I. M. Ferrer, S. M. Chatman, J. C. Peters, T. F. Jaramillo, *J. Am. Chem. Soc.* **2015**, *137*, 4347.
- [29] S. Muhammad-Bashir, M. Al-Oufi, M. Al-Hakami, M. A. Nadeem, K. Mudiyanseelage, H. Idriss, *Sol. Energy* **2020**, *205*, 461.
- [30] T. Maeda, Y. Nagata, N. Endo, M. Ishida, *J. Int. Council Electr. Eng.* **2016**, *6*, 78.
- [31] A. Vilanova, T. Lopes, C. Spenke, M. Wullenkord, A. Mendes, *Energy Storage Mater.* **2018**, *13*, 175.
- [32] V. Andrei, R. L. Hoye, M. Crespo-Quesada, M. Bajada, S. Ahmad, M. De Volder, R. Friend, E. Reisner, *Adv. Energy Mater.* **2018**, *8*, 1801403.
- [33] K. Walczak, Y. Chen, C. Karp, J. W. Beeman, M. Shaner, J. Spurgeon, I. D. Sharp, X. Amashukeli, W. West, J. Jin, N. S. Lewis, C. Xiang, *ChemSusChem* **2015**, *8*, 544.
- [34] M. Schröder, K. Kailasam, J. Borgmeyer, M. Neumann, A. Thomas, R. Schomäcker, M. Schwarze, *Energy Technol.* **2015**, *3*, 1014.
- [35] Y. Goto, T. Hisatomi, Q. Wang, T. Higashi, K. Ishikiriya, T. Maeda, Y. Sakata, S. Oku, H. Tokudome, M. Katayama, S. Akiyama, H. Nishiyama, Y. Inoue, T. Takewaki, T. Setoyama, T. Minegishi, T. Takata, T. Yamada, K. Domen, *Joule* **2018**, *2*, 509.
- [36] K. R. Tolod, S. Hernández, N. Russo, *Catalysts* **2017**, *7*, 13.
- [37] I. Y. Ahmet, Y. Ma, J.-W. Jang, T. Henschel, B. Stannowski, T. Lopes, A. Vilanova, A. Mendes, F. Abdi, R. van de Krol, *Sustainable Energy Fuels* **2019**, *3*, 2366.
- [38] S. A. Lee, I. J. Park, J. W. Yang, J. Park, T. H. Lee, C. Kim, J. Moon, J. Y. Kim, H. W. Jang, *Cell Rep. Phys. Sci.* **2020**, *1*, 100219.
- [39] J.-W. Schüttauf, M. A. Modestino, E. Chinello, D. Lambelet, A. Delfino, D. Dominé, A. Faes, M. Despeisse, J. Bailat, D. Psaltis, C. Moser, C. Ballif, *J. Electrochem. Soc.* **2016**, *163*, F1177.
- [40] J. Gao, F. Sahli, C. Liu, D. Ren, X. Guo, J. Werner, Q. Jeangros, S. M. Zakeeruddin, C. Ballif, M. Graetzel, J. Luo, *Joule* **2019**, *3*, 2930.
- [41] S. Nordmann, B. Berghoff, A. Hessel, N. Wilck, B. Osullivan, M. Debucquoy, J. John, S. Starschich, J. Knoch, *Renewable Energy* **2016**, *94*, 90.
- [42] K. Welter, N. Hamzelui, V. Smirnov, J. P. Becker, W. Jaegermann, F. Finger, *J. Mater. Chem. A* **2018**, *6*, 15968.
- [43] G. Heremans, C. Trompoukis, N. Daems, T. Bosserez, I. F. J. Vankelecom, J. A. Martens, J. Rongé, *Sustainable Energy Fuels* **2017**, *1*, 2061.
- [44] S. Bepalko, A. Kachymov, K. Koberidze, O. Bepalko, *Int. J. Green Sustainable Energy* **2015**, *4*, 182.
- [45] K. Fujii, S. Nakamura, M. Sugiyama, K. Watanabe, B. Bagheri, Y. Nakano, *Int. J. Hydrogen Energy* **2013**, *38*, 14424.
- [46] K. A. Walczak, G. Segev, D. M. Larson, J. W. Beeman, F. A. Houle, I. D. Sharp, *Adv. Energy Mater.* **2017**, *7*, 1602791.
- [47] T. A. Kistler, D. Larson, K. Walczak, P. Agbo, I. D. Sharp, A. Z. Weber, N. Danilovic, *J. Electrochem. Soc.* **2019**, *166*, H3020.
- [48] M. A. Modestino, K. A. Walczak, A. Berger, C. M. Evans, S. Haussener, C. Koval, J. S. Newman, J. W. Ager, R. A. Segalman, *Energy Environ. Sci.* **2014**, *7*, 297.
- [49] J. P. Becker, B. Turan, V. Smirnov, K. Welter, F. Urbain, J. Wolff, S. Haas, F. Finger, *J. Mater. Chem. A* **2017**, *5*, 4818.

- [50] E. Verlage, S. Hu, R. Liu, R. J. Jones, K. Sun, C. Xiang, N. S. Lewis, H. A. Atwater, *Energy Environ. Sci.* **2015**, *8*, 3166.
- [51] C. R. Cox, J. Z. Lee, D. G. Nocera, T. Buonassisi, *Proc. Natl. Acad. Sci.* **2014**, *111*, 14057.
- [52] B. Turan, J.-P. Becker, F. Urbain, F. Finger, U. Rau, S. Haas, *Nat. Commun.* **2016**, *7*, 12681.
- [53] S. Calnan, S. Aschbrenner, F. Bao, E. Kemppainen, I. Dorbandt, R. Schlatmann, *Energies* **2019**, *12*, 4176.
- [54] G. Zhang, Y. Shi, A. Maleki, M. Rosen, *Renewable Energy* **2020**, *156*, 1203.
- [55] M. Kölbach, K. Rehfeld, M. M. May, *Energy Environ. Sci.* **2021**, *14*, 4410.